tvst

DOI: 10.1167/tvst.5.5.12

Article

Quantitative Evaluation of Microdistortions in Bowman's Layer and Corneal Deformation after Small Incision Lenticule Extraction

Rushad Shroff[1], Mathew Francis[2], Natasha Pahuja[1], Leio Veeboy[2], Rohit Shetty[1,3], and Abhijit Sinha Roy[4]

[1] Cornea and Refractive Surgery Division, Narayana Nethralaya, Bangalore, India
[2] Imaging, Biomechanics and Mathematical Modeling Solutions, Narayana Nethralaya Foundation, Bangalore, India
[3] Vice-Chairman, Narayana Nethralaya, Bangalore, India
[4] Chief Scientist, Imaging, Biomechanics and Mathematical Modeling Solutions, Narayana Nethralaya Foundation, Bangalore, India

Correspondence: Abhijit Sinha Roy, Narayana Nethralaya Foundation, #258A Hosur Road, Bommasandra, Bangalore, India-560099. e-mail: asroy27@yahoo.com

Received: 1 April 2016
Accepted: 31 August 2016
Published: 17 October 2016

Keywords: visual impression; vision simulator; visual acuity; diffractive multifocal IOL; trifocal IOL

Citation: Shroff R, Francis M, Pahuja N, Veeboy L, Shetty R, Sinha Roy A. Quantitative evaluation of microdistortions in Bowman's layer and corneal deformation after small incision lenticule extraction. Trans Vis Sci Tech. 2016;5(5):12, doi:10.1167/tvst.5.5.12

Purpose: To quantitatively evaluate microdistortions in Bowman's layer and change in corneal stiffness after small incision lenticule extraction (SMILE).

Methods: This was a prospective, longitudinal, and interventional study. Thirty eyes of 30 patients were screened preoperatively and underwent SMILE for treatment of myopia with astigmatism. Visual acuity, refraction, optical coherence tomography (OCT; Bioptigen, Inc., Morrisville, NC) imaging of the layer and air-puff applanation (Corvis-ST, OCULUS Optikgeräte Gmbh, Germany) was performed before and after surgery (1 day, 1 week, and 1 month). The Bowman's Roughness Index (BRI) was defined as the enclosed area between the actual and an ideal smooth layer to quantify the microdistortions. A viscoelastic model was used to quantify the change in corneal stiffness using applanation.

Results: Uncorrected distance visual acuity improved ($P < 0.001$) and refractive error decreased ($P < 0.0001$) after SMILE. BRI increased from preoperative levels (1.81×10^{-3} mm^2) to 1 week (3.14×10^{-3} mm^2) after SMILE ($P < 0.05$) and then decreased up to a month (2.43×10^{-3} mm^2; $P < 0.05$). Increase in the magnitude of the index correlated positively with refractive error ($P = 0.02$). However, corneal stiffness reduced after SMILE (105.86 $\pm$ 1.4 N/m versus 97.97 $\pm$ 1.21 N/m at 1 month, $P = 0.001$). The decrease in corneal stiffness did not correlate with refractive error ($P = 0.61$).

Conclusions: BRI correlated positively the magnitude of refractive error. However, decrease in corneal stiffness, assessed by air-puff applanation, may not be related to microdistortions after SMILE.

Translational Relevance: An objective method of quantification of Bowman's layer microdistortions using OCT was developed to monitor corneal wound healing and improve lenticule extraction methods.

Introduction

Since the advent of femtosecond lasers in refractive surgery, the predictability of laser-assisted laser in situ keratomileusis (LASIK) flaps has been superior to microkeratome based LASIK flaps.[1] In 2011, a new method called small incision lenticule extraction (SMILE) was reported.[2] Since then several studies have demonstrated comparable refractive outcomes between SMILE and LASIK, with significantly less dryness and inflammation.[3–5] Theoretical biomechanical advantage of SMILE over LASIK was analyzed in recent studies.[6,7] Clinical significance and utility of this biomechanical advantage is yet to be proven (e.g., assessment of ectasia risk).

Recent studies have reported the occurrence of unintended microdistortions in Bowman's layer after SMILE.[8–10] There are several factors related to the induction of microdistortions (e.g., ease of separation and extraction of lenticule from the stroma, corneal biomechanics, refractive error).[11] In this study, a new

index, named Bowman's Roughness Index (BRI), was defined to quantify the microdistortions in the central cornea following SMILE. It was hypothesized that change in BRI would be greater in eyes with greater refractive error. Therefore, correlation between change in BRI and change in refractive error was assessed. BRI quantified the smoothness of the anterior edge of the Bowman's layer and was used for location-specific analyses, without the need for peripheral corneal imaging.[12] A mathematical method using a linear spring-dashpot model to estimate corneal stiffness from air-puff applanation was used for biomechanical analyses.

Methods

Study Population

The study was a prospective, interventional, longitudinal case series. The study was approved by the ethics committee of Narayana Nethralaya Multi-Specialty Eye Hospital, Bangalore, India. Written informed consent was obtained from the patients. The study was conducted in accordance with the tenets of the Declaration of Helsinki. The study included 30 randomly selected eyes of 30 patients, who underwent SMILE. A random sequence of numbers ranging from 1 to 30 was generated by a random number generator and indexed in ascending order (e.g., the first index in the list could be the 10th patient, the second index in the list could be 21st patient and so on). Then, the left eye of all odd indices and the right eye of all even indices were selected for analyses. Patients between 18 to 50 years of age with a stable moderate to high myopia for a minimum period of 1 year (a change of 0.25 D or less), a corrected distance visual acuity (CDVA) of 20/25 or better, a spherical equivalent refraction less than −10 D and a refractive astigmatism less than −3 D were included in the study. Patients with central corneal thickness (CCT) less than 480 μm, a calculated residual stromal bed thickness of less than 250 μm after the surgery, a history of keratoconus, diabetes, collagen vascular disease, pregnancy, breastfeeding, and any prior ocular surgery or trauma were excluded from the study.

Study Design

All patients underwent uncorrected distance visual acuity (UDVA), CDVA, and refraction (sphere and cylinder) assessment before and 1 month after surgery. Corneal deformation was measured with Corvis-ST (OCULUS Optikgeräte Gmbh, Germany) before and 1 month after surgery. Biomechanical measurements were performed only a month after SMILE to allow the cornea to heal and after the application of most topical medications ended other than artificial tears. The central 3-mm Bowman's layer was imaged with the high resolution optical coherence tomography (OCT; Envisu, Bioptigen, Inc., Morrisville, NC). The OCT had a digital axial and lateral resolution of 1.93 μm and 3 μm, respectively. The OCT had an optical resolution of 2.4 μm in tissue, which allowed imaging of the layer with sufficient number of pixels. This resolution was restricted to the 3-mm image scan size only. Thus, image scan size greater than 3 mm was not used in this study. At 1 month after surgery, UDVA, CDVA, sphere, cylinder, and corneal deformation were measured. However, OCT imaging was performed not only at 1 month but also at day 1 and week 1 after surgery to measure the longitudinal changes in the microdistortions.[8] The same examiner performed the OCT imaging of all the eyes and at all time points. At each time point, the scan was performed along the nasal-temporal direction. The location of the 2-D scan was set at each follow-up such that it subdivided visually the en face projection image of the cornea in to nearly two equal halves. Further, at least three 2-D scans were acquired in quick succession at each follow-up time point.

Surgical Procedure

A single experienced surgeon performed all the surgeries using the VisuMax FS laser system (Carl Zeiss Meditec AG, Jena, Germany) with a 500-kHz repetition rate under topical anesthesia (0.5% proparacaine hydrochloride, Sunways Pvt. Ltd., Maharashtra, India) instilled two to three times under aseptic precautions. Laser cut energy index was 170 nJ. Spot spacing was 2 μm for creation of the lenticule side cut and 4.5 μm for creation of the lenticule. Lenticule and cap diameter was 6.0 and 7.7 mm, respectively. Intended cap thickness was 110 μm. After the refractive lenticule was created, it was dissected and separated through the side-cut opening and removed manually. No fluid hydration or intraoperative massaging of the cornea was performed after lenticule removal. At the end of the procedure, the cornea was moistened with a wet merocel sponge. A drop of moxifloxacin hydrochloride 0.5% (Vigamox, Alcon Laboratories, Inc, Fort Worth, TX) was instilled in both eyes and the procedure was completed. Postoperative treatment

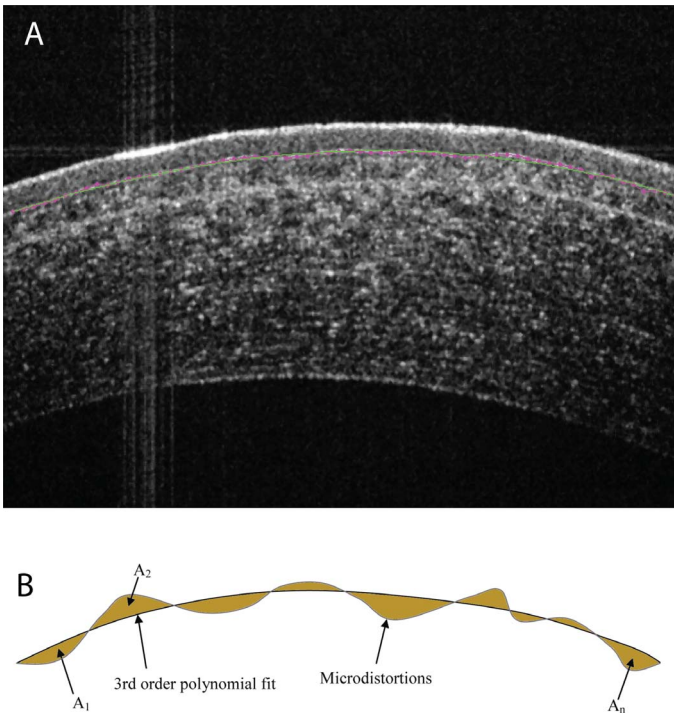

Figure 1. Optical coherence tomography (raw) image of Bowman's layer after SMILE (*top figure*). *Pink line* is the actual Bowman's layer edge and *green line* is curve fit to the *pink line*. Curve fit was performed with a third order polynomial equation on the segmented edge with microdistortions. The shaded areas are shown in the *bottom figure* and represent the areas enclosed between the segmented Bowman's layer edge and the smooth polynomial fit. Bowman Roughness Index is the sum of all the shaded areas in the *bottom figure*.

included 0.5% moxifloxacin hydrochloride four times a day for 1 week, tapering dose of topical 1% prednisolone acetate suspension (Pred Forte, Allergan, Inc., Irvine, CA) starting from four times a day to once daily for 3 days each and a topical lubricant (Optive, Allergan, Inc.) four times a day for a month.

Study Endpoints

The posterior edge of the Bowman's layer became less evident after SMILE. Therefore, only the anterior edge of the Bowman's layer was segmented from the OCT images before and after surgery (pink line in Fig. 1, top) using graph theory (MathWorks, Inc., Natick, MA).[13] After segmentation, a third order polynomial was curve fit to the segmented pixels of the edge (green line in Fig. 1, top). A third order polynomial was chosen since a paraxial second order equation can be used to represent a meridian of most normal corneas.[13] With a third order polynomial, the second order gradient necessary for curvature calculations can be captured better. Since the same order of the polynomial was used before and after SMILE, the spatial resolution of curve fitting method was also the same before and after SMILE. A schematic overlay of the segmented edge of Bowman's layer and third order polynomial curve fit is shown in Figure 1 bottom. The shaded areas represent the areas enclosed between the microdistortions and curve fit. If A_1, A_2, …, A_n were n enclosed areas, BRI was defined as the summation:

$$\mathrm{BRI} = \sum_{k=1}^{n} A_k = A_1 + A_2 + \ldots + A_n \qquad (1)$$

If there were more microdistortions, the magnitude of BRI would increase and vice versa. Further, BRI was zero, when microdistortions were absent. The mean BRI from three images of each eye was calculated and used for further analyses.

To evaluate the corneal deformation before and after surgery, a spring and dashpot model was modified from a recent study[14] to quantify the corneal deformation independent of the extra-ocular tissue deformation. The spring and dashpot model was used to describe the deformation amplitude (reported by Corvis-ST), which was a sum of the cornea and extra-ocular tissue deformation in response to the force applied by the air-puff ($F_{\text{air-puff}}$).[14] The previous study was not able to assess the stiffness of the cornea independently.[14] In this study, the model was improved further by using a combination of a spring, having stiffness Kc (in N/m), and a parallel network, having stiffness Kg (in N/m) and viscosity μg (in Pa.sec). This improved model is shown in Figure 2. The mathematical description that linked $F_{\text{air-puff}}$ and the corneal deformation was as follows:

$$F_{\text{air-puff}} = \mathrm{Kc}(u_1 - u_2) + \mathrm{Kg}(u_2) + \mu\mathrm{g}\left(\frac{du_2}{dt}\right) \qquad (2)$$

In equation (2), Kc represented the stiffness of the cornea. Kg and μg represented the stiffness and viscosity of the extra-ocular tissues, respectively. u_1 was the deformation amplitude waveform reported by Corvis-ST. u_2 was the deformation of the extra-ocular tissues only. The term du_2 / dt accounted for the viscous delay in the deformation of the extra-ocular tissues. Thus, corneal deformation was given by $u_1 - u_2$. By using equation (2), the effect of SMILE on the change in deformation of both the cornea and extra-ocular tissues could be assessed. By measuring the deformation of the segmented anterior edge of the cornea near its endpoints, u_2 was calculated.[15] The

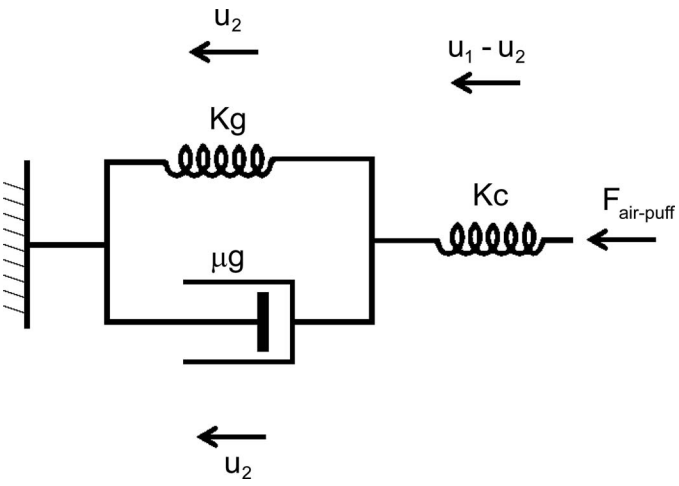

Figure 2. A spring-dashpot model to describe corneal and extra-ocular tissue deformation caused by air-puff applanation. Kc and Kg are the corneal and extra-ocular tissue stiffnesses, respectively. µg is the viscosity of the extra-ocular tissue. u_1 and u_2 are the deformation amplitude and deformation of the extra-ocular tissue, respectively. $F_{\text{air-puff}}$ is the force applied by the air-puff.

stiffness of the cornea varies nonlinearly with applied stress or force.[16] Therefore, Kc was represented as a function of applied air-puff pressure ($P_{\text{air-puff}}$):

$$\text{Kc} = \beta e^{\alpha P_{\text{air-puff}}} \quad (3)$$

Equation (3) simply implied that the cornea stiffened exponentially as the air-puff pressure increased. The cornea is always under stress due to force (F_{IOP}) of the intraocular pressure (IOP) in vivo. During applanation, there was a net force being applied, which can be mathematically represented as F_{IOP}+$F_{\text{air-puff}}$. By treating the in situ configuration of the cornea as the baseline, the corneal deformation during applanation was simply due to $F_{\text{air-puff}}$ (i.e., F_{IOP}+$F_{\text{air-puff}}$ minus F_{IOP}). By combining equations (2) and (3) into equation (4), a unique quantification of the nonlinear corneal stiffness and extra-ocular stiffness plus viscosity was achieved.

$$F_{\text{air-puff}} = \beta e^{\alpha P_{\text{air-puff}}}(u_1 - u_2) + \text{Kg}(u_2) + \mu\text{g}\left(\frac{du_2}{dt}\right) \quad (4)$$

Here, $F_{\text{air-puff}} = P_{\text{air-puff}} \times$ Applanation Area and t was the current applanation time. Applanation area was approximated as a circle of diameter 2.5 mm.[16] Equation (2) was solved for all time points of the applanation period simultaneously. Least squares technique and finite difference method was used to obtain Kc, Kg, and µg. In Corvis-ST, $P_{\text{air-puff}}$ varied from 0 to 180 mmHg. Since $P_{\text{air-puff}}$ varied during applanation, Kc also varied. After β and α were computed from equation (4), Kc was computed at all $P_{\text{air-puff}}$ ranging from 0 to 180 mmHg in steps of 10 mmHg. Mean corneal stiffness ($\widetilde{\text{Kc}}$) was calculated as the mean of all Kcs at corresponding $P_{\text{air-puff}}$. In equation (4), mass inertia of the cornea was neglected as it had negligible impact on the computed values of Kc and $\widetilde{\text{Kc}}$ due to explicit delineation of corneal deformation from the deformation amplitude waveform.[14,16] Both Kc and $\widetilde{\text{Kc}}$ represented a summation effect of both geometry (thickness) and modulus on corneal deformation. Thus if either thickness or modulus or both were effected, it would have also affected Kc and $\widetilde{\text{Kc}}$ (i.e., if thickness was reduced and modulus remained unchanged, corneal stiffness was also reduced). Other corneal deformation variables used for statistical analyses included deformation amplitude at highest concavity, time of first applanation, time of second applanation, time at which highest concavity was attained, area under the deformation amplitude curve,[17] area under the corneal deformation curve,[17] and area under the extra-ocular tissue deformation curve.

Statistical Analysis

All variables were assessed for normality of distribution. Longitudinal group means were assessed with paired t-test and repeated measures analysis of variance with Bonferroni adjustment. Correlation between the ratio of post- to preoperative BRI and change in spherical equivalent was assessed. Similarly, the ratio of post- to preoperative BRI and change in UDVA was assessed. The ratio of post to preoperative BRI would be greater than 1, if microdistortions increased after SMILE and vice versa. The above correlations were also assessed for the ratio of post- to preoperative $\widetilde{\text{Kc}}$. Repeatability of BRI was assessed with coefficient of variation.[18] Coefficient of variation, expressed as percentage, was calculated as the ratio of standard deviation to mean value of BRI from the three images. All variables were presented as mean ± SEM, where SEM was the standard error of the mean. A two-sided P-value < 0.05 was considered statistically significant. Statistical analyses were performed with MedCalc v16.4.3 (MedCalc Software bvba, Ostend, Belgium).

Results

Mean age of the subjects was 24.47 ± 0.67 years. Mean spherical equivalent refractive error was −5.1 ±

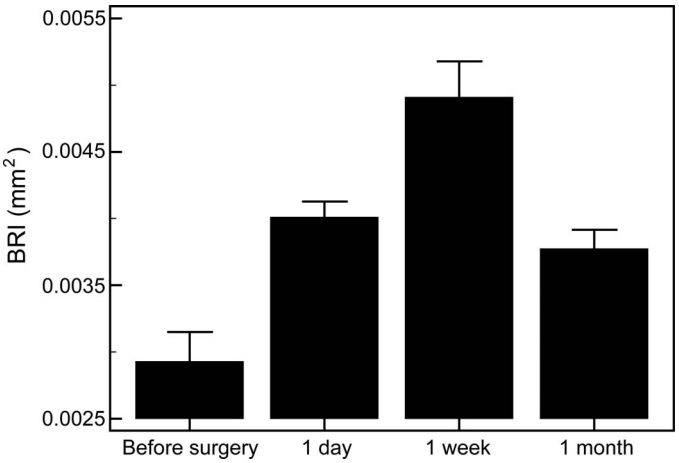

Figure 3. Mean BRI before, 1 day after, 1 week after, and 1 month after surgery. There was a statistically significant difference ($P < 0.0001$) between all time points.

0.3 D and –0.37 ± 0.11 D before and 1 month after SMILE, respectively ($P < 0.0001$). Mean programmed lenticule thickness was 90.68 ± 22.99 μm. Mean CCT was 507.5 ± 4.4 μm and 436.4 ± 7.14 μm before and 1 month after SMILE, respectively ($P < 0.0001$). Mean IOP was 16.7 ± 0.26 and 15.9 ± 0.27 before and 1 month after SMILE, respectively ($P = 0.32$). Mean UDVA (in LogMAR) was 1.06 ± 0.11 and 0.05 ± 0.01 before and 1 month after SMILE, respectively ($P < 0.0001$). Mean CDVA (in LogMAR) was 0.03 ± 0.01 and 0.07 ± 0.02 before and 1 month after SMILE, respectively ($P = 0.34$). All eyes had unchanged CDVA at 1 month ($P > 0.05$).

Mean BRI was $1.86 \times 10^{-3} \pm 6.9 \times 10^{-5}$ mm^2, $2.56 \times 10^{-3} \pm 3.7 \times 10^{-5}$ mm^2, $3.14 \times 10^{-3} \pm 8.5 \times 10^{-5}$ mm^2, and $2.43 \times 10^{-3} \pm 8.5 \times 10^{-5}$ mm^2 before, 1 day after, 1 week after, and 1 month after SMILE, respectively (Fig. 3). The mean ratio of post- to preoperative BRI at 1 day, 1 week, and 1 month after SMILE was 1.40 ± 0.04, 1.64 ± 0.07 and 1.34 ± 0.05, respectively. Mean BRI before surgery was significantly different from mean BRI at day 1 ($P < 0.0001$), week 1 ($P < 0.0001$), and month 1 ($P < 0.0001$). Mean BRI at week 1 was significantly different from mean BRI at day 1 ($P < 0.0001$) and month 1 ($P < 0.0001$) . The coefficient of variation of BRI was 0.1%. The mean coefficient of regression of the third order polynomial curve fit on segmented Bowman's layer edge was $0.99 \pm 1 \times 10^{-3}$. The ratio of post- to preoperative BRI correlated positively with postoperative decrease in spherical equivalent refractive error ($r = +0.51$, $P = 0.02$) and with postoperative improvement in UDVA ($r = +0.38$, $P = 0.03$).

Figure 4 shows an example of measured Corvis-ST data (symbol) and the fitted data from equation (4) (solid line). Figure 4 top left shows a comparison of deformation amplitude measured versus fitted. Similarly, Figure 4 top right, bottom left, and bottom right show a comparison of cornea deformation (measured versus fitted), extra-ocular tissue deformation (measured versus fitted), and applanation pressure (measured versus fitted), respectively. As shown, the model described by equation (4) was able to describe all the measured deformations accurately. In Figures 4B and 4C, the peak corneal and extra-ocular tissue deformation was obtained at ~ 0.015 and ~ 0.02 seconds, respectively. This trend required the use of the term du_2 / dt to model the viscous deformation of the extra-ocular tissues. Figure 5 (top) shows a comparison of Kc versus applanation pressure (symbols) before and 1 month after surgery. The two continuous lines (solid and dashed) in Figure 5 (top) are regressions using equation (3) applied to before and after SMILE data. From Figure 5 (bottom), it is evident that Kc reduced after surgery at all applanation pressures. $\widetilde{\text{Kc}}$ was lower (105.86 ± 1.4 N/m versus 97.97 ± 1.21 N/m) after SMILE ($P = 0.001$). However, the ratio of post- to preoperative $\widetilde{\text{Kc}}$ did not correlate with postoperative decrease in spherical equivalent refractive error ($r = +0.13$, $P = 0.61$) and with postoperative improvement in UDVA ($r = +0.02$, $P = 0.72$) 1 month after SMILE. In these correlations, the same eyes were evaluated before and after surgery. Thus, age and IOP were not potential confounders and change in corneal thickness was highly correlated to attempted refractive correction by design.

Other corneal deformation variables that were significantly altered after SMILE at 1 month were deformation amplitude at highest concavity (1.14 ± 0.01 mm versus 1.22 ± 0.02 mm, $P = 0.001$), time of first applanation (7.53 ± 0.03 msec versus 7.23 ± 0.06 msec, $P = 0.001$), time of second applanation (21.27 ± 0.06 msec versus 21.60 ± 0.08 msec, $P = 0.001$), and time at which highest concavity (14.98 ± 0.08 msec versus 15.20 ± 0.07 msec, $P = 0.001$) was attained. The area under the deformation amplitude curve (13.33 ± 0.22 mm.msec versus 14.73 ± 0.32 mm.msec, $P = 0.001$) and area under the corneal deformation curve (9.94 ± 0.25 mm.msec versus 11.28 ± 0.33 mm.msec, $P = 0.001$) were significantly higher after SMILE indicating increased compliance of the cornea. However, area under extra-ocular tissue deformation curve, Kg and μg were similar before and 1 month after SMILE ($P = 0.73$, 1.0, and

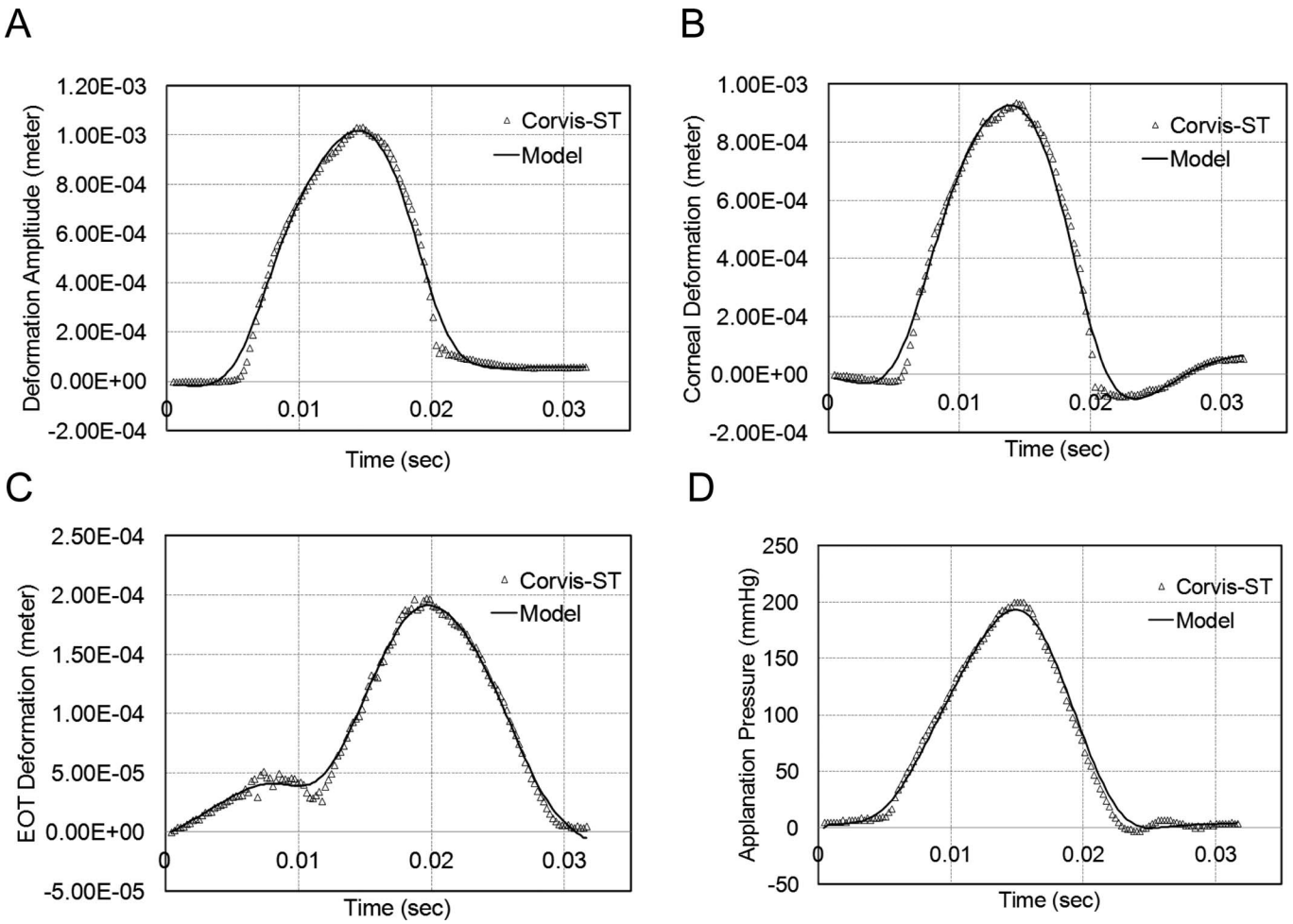

Figure 4. An example of measured versus model fit (described by equation [4]) to deformation amplitude (*top left*), corneal deformation (*top right*), extra-ocular tissue deformation (*bottom left*), and applanation pressure (*bottom right*).

0.73, respectively) indicating that SMILE did not alter extra-ocular tissue deformation.

Discussion

The Bowman's layer does not regenerate, if disrupted, and its degeneration can be a potential marker of specific diseases like keratoconus.[12] Both LASIK and SMILE were designed to preserve the Bowman's layer. In SMILE, microdistortions may be a cause of potential biomechanical instability after the surgery.[8] The earlier study on microdistortions after SMILE used visual examination of the Bowman's layer only to quantify the microdistortions as local peaks.[8] An OCT device was used that had a digital resolution of 5 µm over a scan area of 6 mm.[8] This study improved on the earlier study by using a fully automated image segmentation method to define BRI as a quantifier of microdistortions using high resolution OCT images over a 3-mm scan area. BRI increased and then decreased after SMILE similar to index M.[8] However, an interesting finding was that BRI had a nonzero magnitude before SMILE, which contradicts the assumption of a smooth Bowman's layer preoperatively in the earlier study.[8] Thus, the relative impact of the microdistortions in Bowman's layer on visual quality needs to be assessed with respect to preoperative visual quality in future studies.

Visual examination of microdistortions showed that they remained stable after 1 week and may reduce marginally.[8,10] This study showed that BRI increased up to 1 week and then decreased contrary to the earlier reports.[8,10] The index may serve as a useful metric to quantitatively analyze corneal healing in an individual eye after SMILE. It may also serve as a metric for the surgeons to improve the surgical technique of lenticule separation and extraction to minimize the microdistortions. Surgeons may also

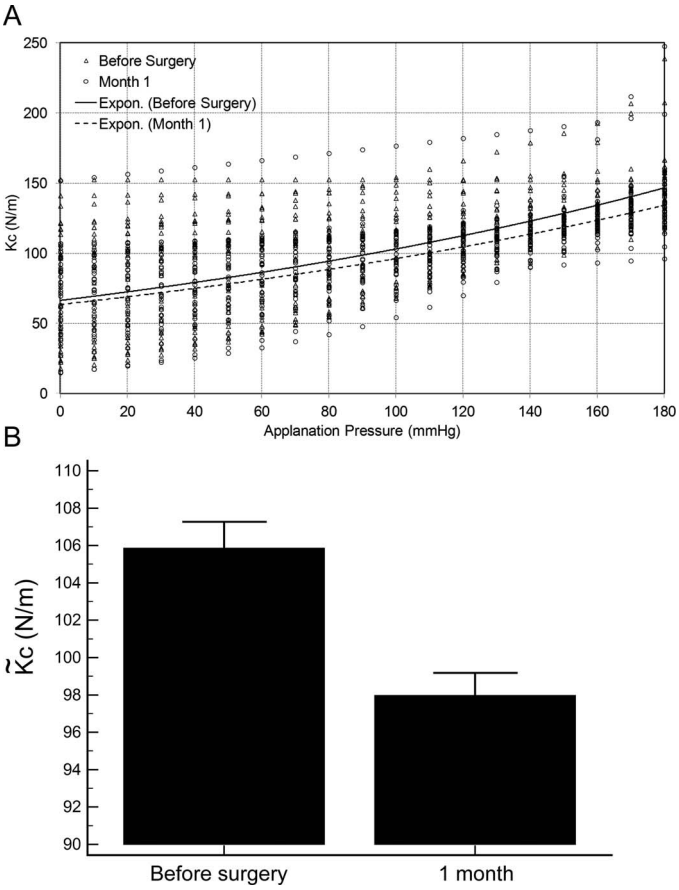

Figure 5. Corneal stiffness versus applanation pressure before and after surgery in all the treated eyes is shown in the *top figure*. The continuous lines are regressions of the preoperative (*solid line*) and postoperative (*dotted line*) data (*top figure*). The *bottom figure* shows the mean corneal stiffness before and 1 month after surgery. * Indicates statistically significant difference ($P = 0.001$) before and after surgery in mean corneal stiffness.

modify the femtosecond laser parameters to deliver optimum energy, which may further reduce the magnitude of the index. Further in eyes where the index does not decrease longitudinally after week 1, there may be unwanted optical complications, which need to be evaluated further.

The ratio of post- to preoperative BRI also correlated positively with the magnitude of refractive correction and change in visual acuity. This implied that the magnitude of microdistortions increased as more tissue was removed. There may be multiple causes of this acute increase in BRI: (a) mechanical stress during lenticule separation[11] and extraction; (b) corneal biomechanics[11]; (c) mismatch between the surface area of the anterior and posterior surface of the lenticule[19]; and (d) relaxation of the anterior lamellae due to severance of the transverse fibers in the anterior stroma.[20] This would cause the anterior lamella to distort acutely and lead to a temporary increase in BRI. It is not clear how these phenomena can be dissociated from each other. Therefore, these phenomena require further study. In this study, a new method of quantification of corneal stiffness (Kc) was also introduced. $\widetilde{K}c$ was significantly lower after SMILE indicating decrease in corneal stiffness. Other biomechanical variables also showed significant alteration after SMILE indicating reduce corneal stiffness (e.g., decrease in time of first applanation indicated that the cornea reached the first applanation point earlier due to thinner cornea and possibly reduced modulus of elasticity). Similarly, increase in area under the corneal deformation curve and unchanged area under the extra-ocular tissue deformation curve indicated an increased compliance of the cornea after SMILE contributed to the increased deformation amplitude. However, the decrease in $\widetilde{K}c$ was independent of the magnitude of refractive error or change in UDVA. Thus, corneal deformation by air-puff applanation was not significantly impacted by the increase in microdistortions or BRI. Further studies with a larger sample size and longer follow-up are needed to validate the results of this study.

Recent studies have investigated the change in corneal deformation after LASIK and SMILE. Corneal deformation parameters reported by Corvis-ST were similar between LASIK and SMILE in a recent study.[21] A study with Ocular response analyzer (ORA) reported decrease in corneal hysteresis (CH) and corneal resistance factor (CRF) after SMILE, but the decrease in magnitude was similar to measurements obtained after LASIK.[22] When the myopic refractive error was > -6 D, the decrease in CH, CRF, and other ORA waveform variables in SMILE eyes were lower than the decrease measured in LASIK eyes.[23] Another study reported that time of first applanation and deformation amplitude were similar after SMILE and LASIK.[24] None of these studies actually reported corneal stiffness nor was the magnitude of any variable delineated from the extra-ocular tissue deformation. Further studies are needed to evaluate $\widetilde{K}c$ in other types of refractive surgery and in degenerate corneas such as keratoconus.

The lack of correlation between the change in $\widetilde{K}c$ and the magnitude of refractive correction also needs to be assessed with long term follow-up. A possible explanation for this lack of correlation may be the level of mechanical stress induced by air-puff appla-

nation.[16,25] Advanced biomechanical models have shown that high air-puff pressure induced high mechanical stresses in the cornea, which can cause the collagen fibers to be recruited.[16,25] Under such a scenario, it becomes complex to segregate the linear (matrix modulus) and nonlinear (collagen modulus) contribution to corneal stiffness by the model used in this study (equation 3).[16,25] Though corneal stiffness was assumed to be a nonlinear function of applanation pressure, better mathematical representation may be needed to capture the nonlinearity of corneal stiffness in future studies. This may enable better biomechanical characterization of the tissue in proportion to the amount of tissue removed and emphasize some biomechanical contribution to the acute increase in BRI.

The present study suggested that the BRI was positively correlated to magnitude of refractive error and remained unaffected by the decrease in corneal stiffness, when assessed by air-puff applanation and viscoelastic model. A limitation of this work was that BRI was analyzed only in scans of the horizontal meridian of the cornea. However, similar magnitude of standard error of the mean at each follow-up time point (Fig. 3) indicated that measurements were repeated at the same location at each follow-up. Three-dimensional quantification of the Bowman's layer may yield additional information about the longitudinal changes after SMILE.[12] However, the low coefficient of variation of BRI and concordance with past studies supported the conclusions from this study. Improved methods[26] and devices[27] for extraction of the lenticule may also reduce the magnitude of BRI after SMILE. This needs to be evaluated further.

Acknowledgments

Funded in part by Carl Zeiss, Inc., Germany and by the SIBAC grant, Indo-German Science and Technology Center, India.

Abhijit Sinha Roy has intellectual property related to computational modeling through Cleveland Clinic Innovations, Cleveland, Ohio. Rohit Shetty and Abhijit Sinha Roy have a pending patent application based on the work presented in this paper. No other author has any financial or proprietary interests to declare.

Disclosure: **R. Shroff**, None; **M. Francis**, None; **N. Pahuja**, None; **L. Veeboy**, None; **R. Shetty**, None; **A. Sinha Roy**, None

References

1. Pajic B, Vastardis I, Pajic-Eggspuehler B, Gatzioufas Z, Hafezi F. Femtosecond laser versus mechanical microkeratome-assisted flap creation for LASIK: a prospective, randomized, paired-eye study. *Clin Ophthalmol*. 2014;8:1883–1889.
2. Sekundo W, Kunert KS, Blum M. Small incision corneal refractive surgery using the small incision lenticule extraction (SMILE) procedure for the correction of myopia and myopic astigmatism: results of a 6-month prospective study. *Br J Ophthalmol*. 2011;95:335–339.
3. Moshirfar M, McCaughey MV, Reinstein DZ, et al. Small-incision lenticule extraction. *J Cataract Refract Surg*. 2015;41:652–665.
4. Xu Y, Yang Y. Dry eye after small incision lenticule extraction and LASIK for myopia. *J Refract Surg*. 2014;30:186–190.
5. Denoyer A, Landman E, Trinh L, Faure JF, Auclin F, Baudouin C. Dry eye disease after refractive surgery: comparative outcomes of small incision lenticule extraction versus LASIK. *Ophthalmology*. 2015;122:669–676.
6. Reinstein DZ, Archer TJ, Randleman JB. Mathematical model to compare the relative tensile strength of the cornea after PRK, LASIK, and small incision lenticule extraction. *J Refract Surg*. 2013;29:454–460.
7. Sinha Roy A, Dupps WJ Jr, Roberts CJ. Comparison of biomechanical effects of small-incision lenticule extraction and laser in situ keratomileusis: finite-element analysis. *J Cataract Refract Surg*. 2014;40:971–980.
8. Luo J, Yao P, Li M, et al. Quantitative analysis of microdistortions in Bowman's layer using optical coherence tomography after SMILE among different myopic corrections. *J Refract Surg*. 2015;31:104–109.
9. Zhao Y, Li M, Yao P, Shah R, Knorz MC, Zhou X. Development of the continuous curvilinear lenticular rhexis technique for small incision lenticule extraction. *J Refract Surg*. 2015;31:16–21.
10. Yao P, Zhao J, Li M, Shen Y, Dong Z, Zhou X. Microdistortions in Bowman's layer following femtosecond laser small incision lenticule extraction observed by Fourier-Domain OCT. *J Refract Surg*. 2013;29:668–674.

11. Shetty R, Kaweri L, Pahuja N, Deshpande K, Thakkar M, Sinha Roy A. Association between corneal deformation and ease of lenticule separation from residual stroma in small incision lenticule extraction. *Cornea*. 2015;34:1067–1071.
12. Abou Shousha M, Perez VL, Fraga Santini Canto AP, et al. The use of Bowman's layer vertical topographic thickness map in the diagnosis of keratoconus. *Ophthalmology*. 2014;121:988–993.
13. McNabb RP, Farsiu S, Stinnett SS, Izatt JA, Kuo AN. Optical coherence tomography accurately measures corneal power change from laser refractive surgery. *Ophthalmology*. 2015;122:677–686.
14. Han Z, Tao C, Zhou D, et al. Air puff induced corneal vibrations: theoretical simulations and clinical observations. *J Refract Surg*. 2014;30:208–213.
15. Koprowski R, Ambrósio R Jr, Reisdorf S. Scheimpflug camera in the quantitative assessment of reproducibility of high-speed corneal deformation during intraocular pressure measurement. *J Biophotonics*. 2015;8:968–978.
16. Sinha Roy A, Kurian M, Matalia H, Shetty R. Air-puff associated quantification of non-linear biomechanical properties of the human cornea in vivo. *J Mech Behav Biomed Mater*. 2015;48:173–182.
17. Shetty R, Nuijts RM, Srivatsa P, et al. Understanding the correlation between tomographic and biomechanical severity of keratoconic corneas. *Biomed Res Int*. 2015;2015:294197.
18. Shetty R, Arora V, Jayadev C, Nuijts RM, et al. Repeatability and agreement of three Scheimpflug-based imaging systems for measuring anterior segment parameters in keratoconus. *Invest Ophthalmol Vis Sci*. 2014;55:5263–5268.
19. Charman WN. Mismatch between flap and stromal areas after laser in situ keratomileusis as source of flap striae. *J Cataract Refract Surg*. 2002;28:2146–2152.
20. Winkler M, Shoa G, Xie Y, et al. Three-dimensional distribution of transverse collagen fibers in the anterior human corneal stroma. *Invest Ophthalmol Vis Sci*. 2013;54:7293–7301.
21. Pedersen IB, Bak-Nielsen S, Vestergaard AH, et al. Corneal biomechanical properties after LASIK, ReLEx flex, and ReLEx smile by Scheimpflug-based dynamic tonometry. *Graefes Arch Clin Exp Ophthalmol*. 2014;252:1329–1335.
22. Agca A, Ozgurhan EB, Demirok A, et al. Comparison of corneal hysteresis and corneal resistance factor after small incision lenticule extraction and femtosecond laser-assisted LASIK: a prospective fellow eye study. *Cont Lens Anterior Eye*. 2014;37:77–80.
23. Wang D, Liu M, Chen Y, et al. Differences in the corneal biomechanical changes after SMILE and LASIK. *J Refract Surg*. 2014;30:702–707.
24. Shen Y, Chen Z, Knorz MC, Li M, Zhao J, Zhou X. Comparison of corneal deformation parameters after SMILE, LASEK, and femtosecond laser-assisted LASIK. *J Refract Surg*. 2014;30:310–318.
25. Matalia J, Francis M, Tejwani S, Dudeja G, Rajapa, N, Sinha Roy A. Role of age and myopia in simultaneous assessment of corneal and extraocular tissue stiffness by air-puff applanation. *J Refrac Surg*. 2016;32:486–493.
26. Zhao Y, Li M, Yao P, et al. Development of the continuous curvilinear lenticulerrhexis technique for small incision lenticule extraction. *J Refract Surg*. 2015;31:16–21.
27. Liu YC, Pujara T, Mehta JS. New instruments for lenticule extraction in small incision lenticule extraction (SMILE). *PLoS One*. 2014;9:e113774.